

Surface Urban Heat Island Across 419 Global Big Cities

Shushi Peng,[†] Shilong Piao,^{*,†,‡} Philippe Ciais,[§] Pierre Friedlingstein,^{||} Catherine Ottle,[§] François-Marie Bréon,[§] Huijuan Nan,[†] Liming Zhou,[#] and Ranga B. Myneni[⊥]

[†]College of Urban and Environmental Sciences, Peking University, Beijing 100871, China

[‡]Institute of Tibetan Plateau Research, Chinese Academy of Sciences, Beijing 100085, China

[§]Laboratoire des Sciences du Climat et de l'Environnement, CEA CNRS UVSQ, 91191 Gif-sur-Yvette, France

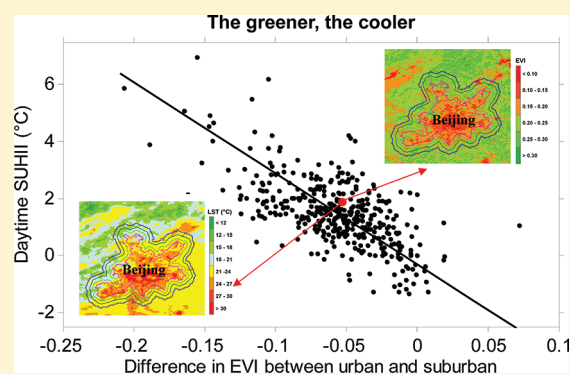
^{||}School of Engineering, Computing and Mathematics, University of Exeter, Exeter EX4 4QF, U.K.

[#]Department of Atmospheric and Environmental Sciences, University at Albany State University of New York, 1400 Washington Avenue Albany, NY 12222, United States

[⊥]Department of Geography and Environment, Boston University, Boston, Massachusetts 02215, United States

S Supporting Information

ABSTRACT: Urban heat island is among the most evident aspects of human impacts on the earth system. Here we assess the diurnal and seasonal variation of surface urban heat island intensity (SUHII) defined as the surface temperature difference between urban area and suburban area measured from the MODIS. Differences in SUHII are analyzed across 419 global big cities, and we assess several potential biophysical and socio-economic driving factors. Across the big cities, we show that the average annual daytime SUHII (1.5 ± 1.2 °C) is higher than the annual nighttime SUHII (1.1 ± 0.5 °C) ($P < 0.001$). But no correlation is found between daytime and nighttime SUHII across big cities ($P = 0.84$), suggesting different driving mechanisms between day and night. The distribution of nighttime SUHII correlates positively with the difference in albedo and nighttime light between urban area and suburban area, while the distribution of daytime SUHII correlates negatively across cities with the difference of vegetation cover and activity between urban and suburban areas. Our results emphasize the key role of vegetation feedbacks in attenuating SUHII of big cities during the day, in particular during the growing season, further highlighting that increasing urban vegetation cover could be one effective way to mitigate the urban heat island effect.



1. INTRODUCTION

Urbanization is among the most evident aspects of human impact on the earth system.¹ It is well-known that urban centers experience higher temperatures than surrounding suburban and rural areas, a phenomenon known as the urban heat island effect.^{2–8} As urbanization is accelerating across the world,⁹ especially in developing countries such as China and India,^{9–11} this urban heat island effect has gained in importance.^{3,4} In the context of global warming it has been suggested that warming trends observed at continental weather stations could be partly influenced by local urban heat islands, thus reducing the contribution of greenhouse gases to global warming,⁵ although this has been disputed by several studies.⁶ On the other side, urban heat island also has negative impacts on the quality of the city life from the aspects of energy consumption, air and water quality, and human health.¹² Therefore, better understanding the drivers of urban heat island intensity is of critical importance for climate research and impacts studies, which has strong implications for urban planning.^{12,13}

Urban heat island intensity is often quantified by the difference in air temperature between a weather station located

in an urban center and one in a less urbanized outskirts,^{7,8} which is usually called air urban heat island.¹³ Because the density of *in situ* weather station networks is sparse and potentially influenced by very local conditions, it is difficult to rely on these data alone for obtaining information about urban heat island at the spatial scale of a city. Satellite remote sensing now offers the opportunity to characterize spatial and temporal structures of land surface temperature (LST),¹⁴ with sufficient resolution to distinguish between urban centers and rural surroundings (Figure 1).^{15,16} Remote sensing LST difference between urban and suburban areas is usually defined as surface urban heat island.^{13,14} Until now, there are many studies using satellite-derived LST to study surface urban heat island focusing on single or several big cities over a region,^{15,17,18} as more satellite products are available such as MODerate-resolution Imaging Spectroradiometer (MODIS) LST and Landsat TM/ETM+.

Received: August 31, 2011

Revised: December 5, 2011

Accepted: December 5, 2011

Published: December 5, 2011

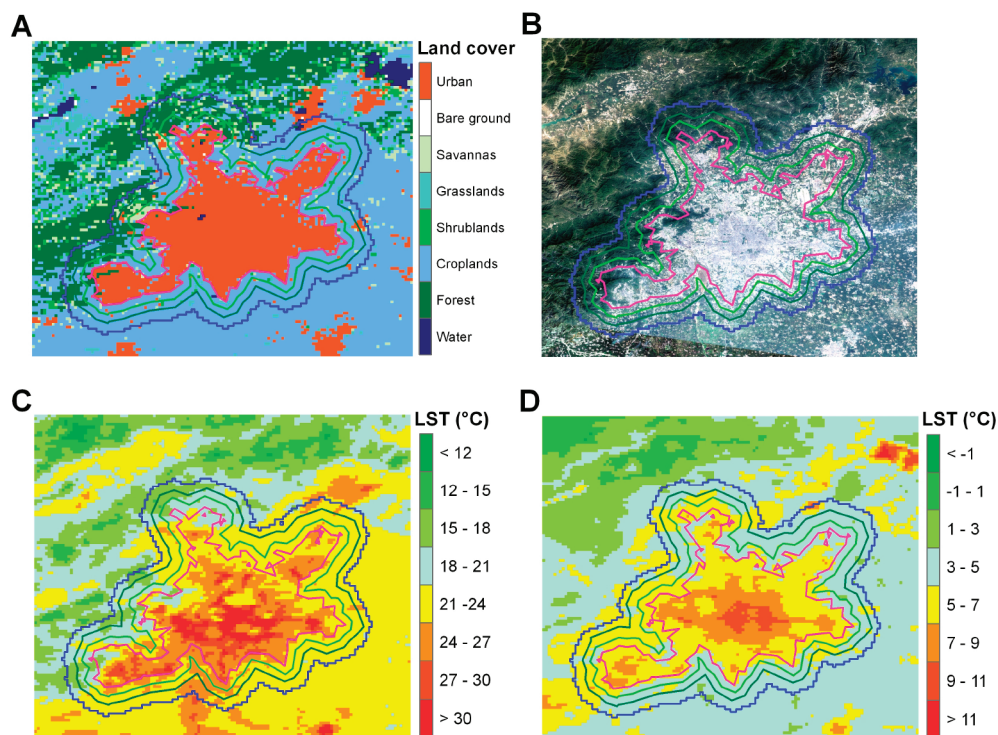


Figure 1. Beijing area maps of (A) MODIS data derived land cover/use, (B) Landsat ETM+ true color image with spatial resolution 30 m × 30 m in August, 2005, (C) annual mean daytime land surface temperature (LST) (°C), and (D) annual mean nighttime LST (°C). The magenta, green, dark green, and blue lines stand for the borders of Beijing urban areas, suburban with 50% of urban areas, suburban with 100% of urban areas, and suburban with 150% of urban areas, respectively.

For example, Hung et al. (2006)¹⁷ used MODIS LST to report 18 Asian mega cities surface urban heat island which is correlated with city population, building up density and vegetation cover. Imhoff et al. (2010)¹⁵ also indicated that there is diurnal and seasonal cycle of surface urban heat island and summer surface urban heat island (4.3 °C) is larger than winter surface urban heat island (1.3 °C) over 38 most populous cities across USA using MODIS LST. However, a systematic evaluation of surface urban heat island for the global big cities using a common method is still missing.

In this study, we use the latest Version 5 of Land Surface Temperature (LST) data set from the EOS-Aqua-MODIS (MODIS-Aqua) during the period 2003–2008 to determine the intensity of the surface urban heat island over 419 big cities (with a population of more than 1 million). The primary objective is to quantify the diurnal, seasonal variations, and between-city differences in surface urban heat island and to gain insights on its linkage to biophysical drivers such as vegetation greenness, albedo and mean climate, and to socio-economic drivers such as nighttime lights and population density. We separate the analysis of urban heat island mechanisms between daytime and nighttime.

2. DATA SETS AND METHODS

2.1. Data Sets. Land Surface Temperature (LST) data at a spatial resolution of 1 km and 8-day interval was obtained from EOS-Aqua-MODIS V5 composite products (MYD11A2). The LST data include daytime (~13:30) and nighttime (~01:30) temperature observations from 2003 to 2008. The retrieval of surface temperature was further improved by correcting noise due to cloud contamination, topographic differences, and zenith angle changes.¹⁶ Data quality assessed by Wan (2008)¹⁶

indicates that the MODIS V5 LST are consistent with *in situ* LST measurements, within a root mean squares difference of less than 0.5 K across 39 tested cases. In addition, Wang et al. (2007)¹⁸ reported high accuracy of MODIS LST products on Beijing city based on the surface emissivity evaluations.

We selected 428 big cities with a population larger than 1 million according to population data for year 2007.¹⁹ The location of each big city was determined from a geographical database.²⁰ Urban and nonurban areas over each city were separated according to the MODIS Global Land Cover Map²¹ at 1 km spatial resolution, consistent with the LST data.

To explore the global drivers of surface urban heat islands, we combine satellite observations of vegetation index, albedo, climate, and several socio-economic indexes. The contrast of vegetation and albedo between urban area and suburban area are defined using the MODIS Vegetation Continuous Fields (VCF, essentially the tree cover fraction), the Enhanced Vegetation Index (EVI), and the Bidirectional Reflectance Distribution Function (BRDF) albedo data, respectively. The VCF data are available at 1 km spatial resolution for year 2004,²² and the EVI data at 1 km spatial resolution and 16-day interval are available from 2003 to 2008.²³ The MODIS albedo products used in this study include black sky albedo (BSA) and white sky albedo (WSA) over shortwave broadband (0.3–5.0 μm) with 1 km spatial resolution and 8-day interval for year 2005.²⁴ The climate data including air temperature and precipitation are derived from Climatic Research Unit (CRU) TS3.0 data sets with 0.5° spatial resolution during the period 1971–2000.²⁵

The population density of each city and its suburban area were extracted from the Gridded Population of the World Version 3 (GPWv3) provided by the Center for International

Earth Science Information Network of Columbia University.²⁶ This data set is based on UN population statistics in 2005, with a spatial resolution of 2.5'. Finally, remotely sensed nighttime light data, formerly recognized as a proxy of socio-economic activities^{27,28} were compiled for each urban and suburban area from the stable nighttime light Version 4 data set,²⁹ the latest version produced by the NOAA National Geophysical Data Center (NGDC). This nighttime light data set spans the period from 2003 to 2008, at a spatial resolution of 30".

2.2. Analyses. We define the Surface Urban Heat Island Intensity (SUHII) as the difference of land surface temperature between urban area and suburban area. For each city, we calculate the difference of urban LST minus suburban LST. Urban area is determined by the City Clustering Algorithm,³⁰ according to the MODIS land cover map (see detailed algorithm of city clustering in the Supporting Information (SI)). Since the City Clustering Algorithm could not be successfully applied in 9 cities of the tropical regions (because urban pixels are very discrete), we analyzed only 419 of 428 cities in this study (Table S1). After urban area is determined, suburban area is defined as all of the nonurban pixels (excluding water pixels) within the ring zone around the urban area, which covers the same amount of land as urban area. To test the impact of different suburban area definitions on SUHII, we also showed similar results from a smaller suburban area (as 50% of the urban area) and a larger suburban area (as 150% of the urban area) (Figure 1, SI Figure S1). Daytime and nighttime SUHII were calculated separately from EOS-Aqua-MODIS LST in the early afternoon (~13:30) and at night (~01:30), respectively.¹⁶ Both seasonal and annual averaged daytime and nighttime SUHII were computed. The spatial differences of SUHII among big cities are studied during the period 2003–2008.

In parallel with daytime and nighttime SUHII, we define two vegetation parameters, two albedo parameters, three climate parameters, and two density parameters for each big city. The greening parameters are calculated as the VCF difference (δVCF) and the EVI difference (δEVI) between urban and suburban pixels. The albedo parameters are estimated by the difference between urban and suburban pixels in (1) the black sky albedo (δBSA) and (2) the white sky albedo (δWSA) (BSA is linear with WSA and shows similar results to WSA, so only WSA is shown here). The climate parameters for each big city including mean annual air temperature (MAT), mean annual precipitation (MAP), and mean air temperature for the months when air temperature exceeds 0 °C (MT0) were extracted from CRU TS3.0 data sets. Note that such climate parameters may indirectly explain the spatial patterns of SUHII through explaining the conditions of variable intensities of SUHII. The density parameters are estimated by the difference between urban and suburban pixels in (1) the nighttime light intensity difference (δNL) and (2) the population density difference (δPD) between urban and suburban pixels. In order to identify the drivers of daytime and nighttime SUHII, the six predictor variables, δVCF , δEVI , δBSA , δWSA , δNL , and δPD , were regressed against SUHII using the major axis Model II regressions.³¹ Across the Northern Hemisphere, summer is defined as the period from June to August (JJA), while winter is defined as the period from December to February (DJF). In the Southern Hemisphere, summer is defined as the period from December to February (DJF), while winter is defined as the period from June to August (JJA).

3. RESULTS AND DISCUSSION

Figure 2 shows that the annual mean daytime SUHII is positive over most cities (92%). The city of Medellín (Colombia) has a

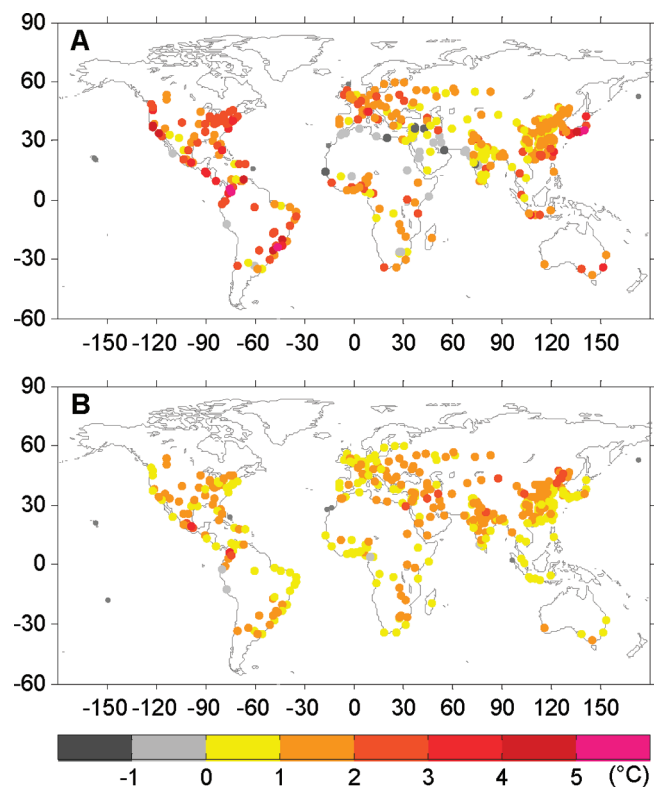


Figure 2. Spatial distribution of (A) annual mean daytime SUHII (°C) and (B) annual mean nighttime SUHII (°C) averaged over the period 2003–2008 across 419 global big cities.

record positive daytime SUHII of 7.0 °C, followed by Tokyo (Japan), Nagoya (Japan), São Paulo (Brazil), and Bogotá (Columbia) (>5 °C). Only a few cities surrounded by desert, such as Jeddah in Saudi-Arabia and Mosul in Iraq, show a negative daytime SUHII. In these places, the inner-city daytime temperature is lower than the surrounding desert (Figure 2A). This feature could be due to evaporative cooling by the vegetation of urban area.³² The annual nighttime SUHIIs over most (95%) of the 419 big cities are between 0 and 2 °C (Figure 2B), and Mexico City has the record high nighttime SUHII of 3.4 °C.

Table 1 summarizes the average annual, summer and winter SUHII across six continents. The average annual daytime and nighttime SUHII is largest in South America and then North America, while Africa shows the lowest annual daytime and nighttime SUHII (Table 1; Figure 2). If the 419 big cities were divided into developed and developing countries based on the United Nations Framework Convention on Climate Change Annex I and II, we found that the annual daytime SUHII over developed countries (2.1 ± 1.1 °C, $n = 116$) is significantly higher than that over developing countries (1.3 ± 1.1 °C, $n = 303$) ($P < 0.001$), but the annual nighttime SUHII over developed countries (1.0 ± 0.4 °C) is close to annual nighttime SUHII over developing countries (1.1 ± 0.6 °C) ($P = 0.014$). The annual SUHII during nighttime (1.1 ± 0.5 °C, $n = 419$), as displayed in Figure 2B and Table 1, is on average lower than that during daytime (1.5 ± 1.2 °C, $n = 419$) ($P < 0.001$). Yet,

Table 1. Annual, Summer, and Winter Daytime and Nighttime Surface Urban Heat Island Intensity (SUHII, °C, Mean \pm SD) across Six Continents (Africa, Asia, Europe, North America, South America, Oceania) Continents and the World^a

	Africa	Asia	Europe	North America	South America	Oceania	World
N	47	209	56	37	65	5	419
annual daytime SUHII (°C)	0.9 \pm 1.1	1.2 \pm 1.0	2.0 \pm 0.9	2.3 \pm 1.6	2.4 \pm 1.0	1.5 \pm 0.7	1.5 \pm 1.2
annual nighttime SUHII (°C)	0.9 \pm 0.5	1.1 \pm 0.5	0.8 \pm 0.4	0.9 \pm 0.7	1.1 \pm 0.5	1.0 \pm 0.4	1.1 \pm 0.5
summer daytime SUHII (°C)	1.0 \pm 1.3	1.5 \pm 1.3	2.1 \pm 1.5	2.5 \pm 1.6	3.0 \pm 1.4	2.3 \pm 1.2	1.9 \pm 1.5
summer nighttime SUHII (°C)	0.7 \pm 0.5	1.0 \pm 0.5	1.0 \pm 0.4	1.0 \pm 0.7	1.3 \pm 0.4	1.3 \pm 0.4	1.0 \pm 0.5
winter daytime SUHII (°C)	0.8 \pm 1.2	0.9 \pm 1.0	1.7 \pm 0.4	2.2 \pm 1.8	1.7 \pm 1.1	0.8 \pm 0.5	1.1 \pm 1.2
winter nighttime SUHII (°C)	1.1 \pm 0.5	1.2 \pm 0.7	0.4 \pm 0.4	0.9 \pm 0.8	0.9 \pm 0.7	0.8 \pm 0.4	1.0 \pm 0.7

^aN is the number of big cities in each continent and the world included in the study.

36% of the cities have a more intense heat island during the night, specifically in western and southern Asia and northern Africa (Figure 2B).

There is no correlation between daytime and nighttime annual SUHII across cities (Figure 3; $R^2 = 0.00$, $P = 0.84$). This

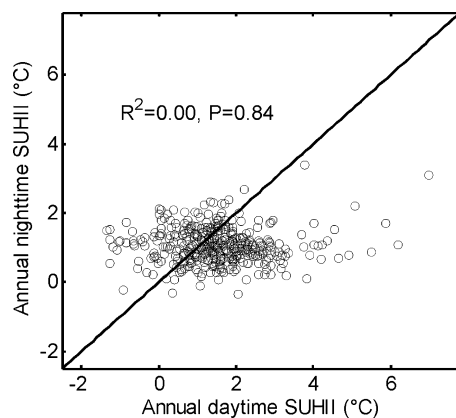


Figure 3. Relationship between annual mean daytime SUHII (°C) and annual mean nighttime SUHII (°C) averaged over the period 2003–2008 across 419 global big cities.

suggests that the factors driving heat islands during the day are different than those at night, and that there is little inertia of daytime processes into the following night. Oke (1988),² followed by Arnfield (2003),¹³ analyzed the drivers of urban heat island by the contrast of surface energy exchange between urban and suburban areas. Downward net solar radiation and anthropogenic heat flux produced by appliances, building heating and light, humans, combustion engines, and transportation constitute the two major sources of energy available to cause urban heat island. These sources of energy are converted into sensible heat fluxes, latent heat fluxes, surface heat storage, and net heat advection.^{2,13}

During the day, generally, sensible heat fluxes and latent heat fluxes mainly derived from net solar radiation are the largest upward heat fluxes.^{2,14,33} The incoming solar energy partitioning between latent heat flux and sensible heat flux is modulated by vegetation fractional coverage and its ability to transpire soil–water per unit of vegetated area. Therefore, vegetation transpiration is expected to produce a cooling effect on surface temperature (Figure 1C). The data presented in Figure 4A lend support to this mechanism, because the difference of vegetation fractional cover (δVCF) and of vegetation activity (δEVI) in urban areas compared to suburban areas is negatively correlated with the daytime heat island across cities, for a wide range of climate zones and environments (δVCF , $R^2 = 0.51$, $P < 0.001$;

δEVI , $R^2 = 0.38$, $P < 0.001$; SI Figure S2). More detailed local studies in Beijing, Tokyo, Seoul, and Indianapolis^{17,34} also found negative correlations between the Normalized Difference Vegetation Index (NDVI) and urban surface temperatures, suggesting the role of urban vegetation in lowering temperatures over urban areas. In addition, it is also reported that a decrease in urban vegetation fraction by 16% could increase urban land surface temperature by 2.5 °C in Guangzhou, China from 1990 to 2007.³⁵

On the other hand, the distribution of nighttime SUHII among cities does not seem to be related to vegetation (Figure 4A and B), which is logical given the absence of vegetation evaporative cooling during the night. During the night, the energy flux from the surface to the atmosphere is the sum of heat stored during the previous day and released at night and of anthropogenic heat produced during the night by the city. The anthropogenic heat flux is related to the energy efficiency of appliances, transportation systems and infrastructures, and to human population density as well.^{33,36,37}

The surface heat storage is related to solar energy absorption (albedo) and thermal properties (heat capacity and thermal conductivity) of the urban surfaces (building density, height, materials, and pavement materials) during the day. It is emitted upward to the atmosphere during the night, contributing to maintain elevated temperatures over urban areas. We found a negative correlation between nighttime SUHII and the albedo difference between urban and suburban areas (δWSA) as displayed by Figure 4A ($R^2 = 0.17$, $P < 0.001$, SI Figure S3) which tentatively suggests a role of surface heat storage in controlling nighttime SUHII. Further in Figure 4A, the spatial correlation between nighttime SUHII and albedo contrast (δWSA) is mainly due to cities whose urban area has a smaller EVI and smaller albedo than the suburban area, i.e. which can potentially absorb solar light and release it subsequently as surface heat storage and sensible heat flux (61% cities in 419 cities). We also found that the albedo contrast δWSA is positively correlated with daytime SUHII ($R^2 = 0.10$, $P < 0.001$) (Figure 4A; SI Figure S2). However, a stepwise multiple linear regression analysis using daytime SUHII as the dependent variable and all independent variables in Figure 4 suggests that daytime SUHII is weakly explained by δWSA (Figure 4B, R^2 is only enhanced by 0.02).

Because direct anthropogenic heat flux by the city during the night should also contribute to maintain nighttime SUHII,^{37,38} we formulated the hypothesis that a proxy for energy emission,^{27,28} namely nighttime light (NL) measured from space, can explain the differences in nighttime SUHII differences between cities. About 13% of the between-city variance of nighttime SUHII is explained by the NL contrast between urban areas and suburban areas (δNL) (Figure 4B).

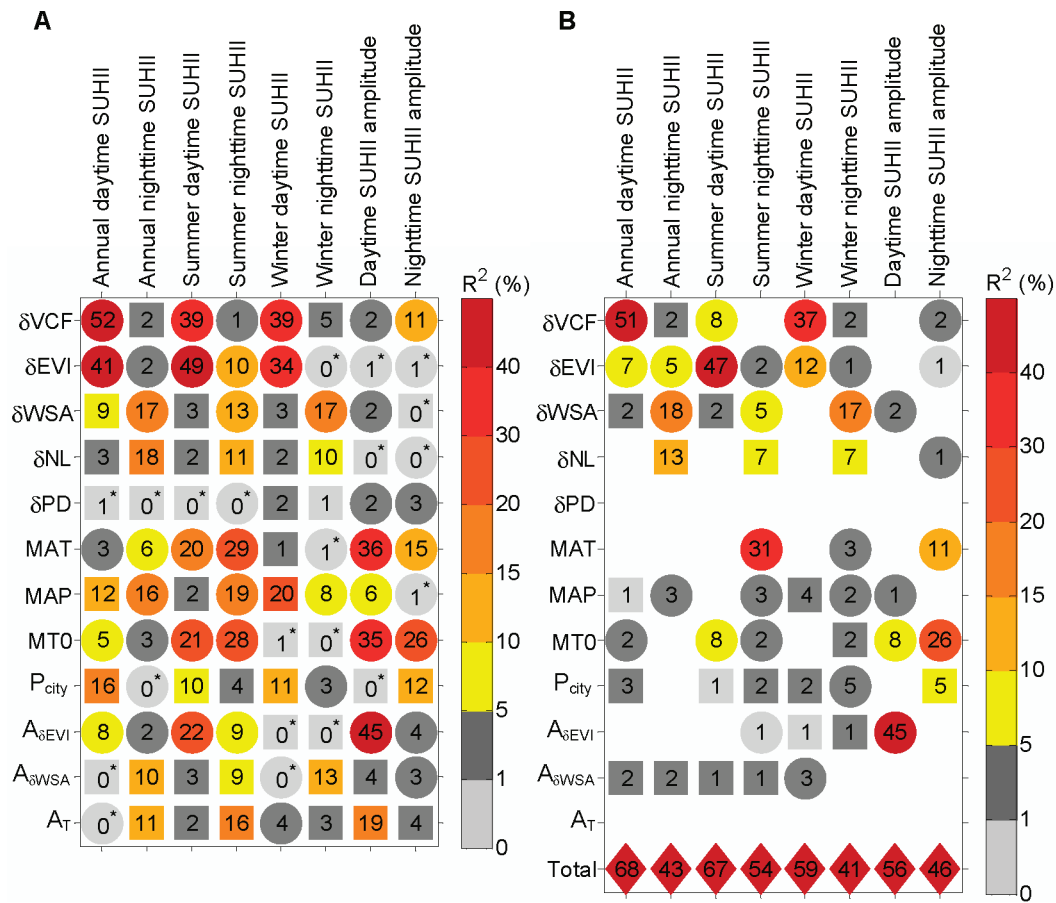


Figure 4. (A) The square of linear correlation coefficients (R^2) of annual daytime and nighttime SUHII and its seasonal amplitude with each variable and (B) stepwise multiple linear regression derived explanation of each variable on the spatial gradient of annual, summer (June-August (JJA) in Northern Hemisphere and December-February (DJF) in Southern Hemisphere), and winter (DJF in Northern Hemisphere and JJA in Southern Hemisphere) daytime and nighttime SUHII as well as its seasonal amplitude (the difference between summer and winter) across 419 cities. The independent variables are as follows: MAT, MAP, MTO, and P_{city} stand for mean annual air temperature, mean annual precipitation, mean temperature for the months when air temperature exceeds 0 °C, and area of the urban area; δVCF , δEVI , δWSA , δNL , and δPD stand for the difference between urban area and suburban area for VCF (δVCF), EVI (δEVI), white sky albedo (δWSA), nighttime light (δNL), and population density (δPD); $A_{\delta EVI}$, $A_{\delta WSA}$, and A_T stand for the average difference between summer and winter for δEVI , δWSA , and air temperature, respectively. Square and circle backgrounds indicate that positive and negative correlation, respectively. A diamond background indicates the total explanation (R^2) of stepwise regression. An asterisk (*) indicates statistically nonsignificant ($P > 0.05$).

δNL , however, does not explain daytime SUHII differences between cities (Figure 4A; $R^2 = 0.01$), most likely because the anthropogenic heat flux is dwarfed during daytime by sensible heat and latent heat emissions.^{2,12,37}

We also tested whether the heat islands of cities are related to their population density and their size. Figure 4 shows that SUHII difference between cities is not explained by the difference in population density (δPD) between urban areas and suburban areas. This indicates that metabolic heating, about 100 W per person,³⁷ accounts for only a very small fraction of the urban anthropogenic heat flux.³⁷ Finally, there is no obvious effect of city size: the urban area of each city obtained from MODIS land cover²¹ explains less than 3% of heat island differences between cities on global scale (Figure 4B). Previous studies found larger urban heat island intensity in bigger cities^{2,15} in one country or region. In our study, because the 419 big cities are from different countries, different climatic zones, and different economic development, the effects of city size on SUHII could be masked by these factors. If the 56 European cities are extracted to test the relationship between

city size and SUHII, city size shows a significant and positive correlation with annual daytime SUHII ($R^2 = 0.16$, $P = 0.003$).

Except for albedo and nighttime light, city structure such as building density, height, and surface materials could also affect the nighttime surface energy exchange, thus impact the nighttime SUHII.^{14,17} This is the possible reason why albedo and nighttime light could only explain part of the spatial variation of nighttime SUHII ($R^2 = 0.17$ for albedo, $R^2 = 0.12$ for nighttime light) across 419 big cities in our study. During the daytime, evapotranspiration depends on both vegetation and soil moisture, hence, soil moisture could also be related to SUHII. Unfortunately, there are no global uniform and high resolution data sets to test the impacts of these physical variables on nighttime SUHII. Future studies need to focus on the most important physical variables related to surface energy exchange and study the processes and mechanisms of urban heat islands using detailed observations and models for a single or several typical cities.

The heat island intensity also varies seasonally.^{15,18} The summer to winter amplitude of SUHII is shown in Figure 5. Daytime SUHII has larger summer to winter amplitude than

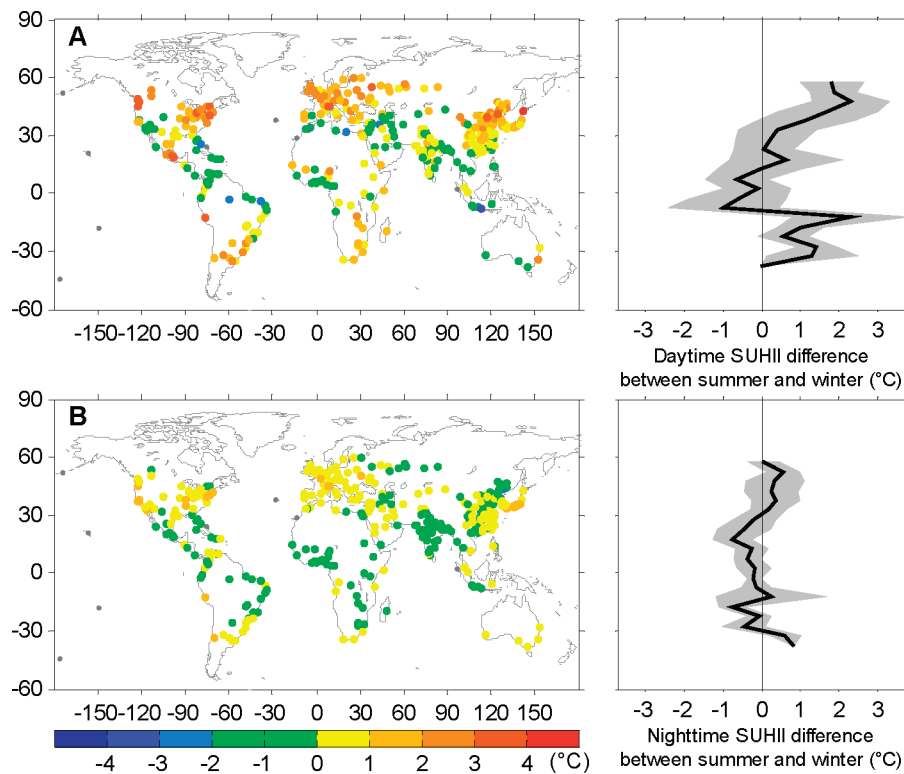


Figure 5. Spatial distribution of (A) average daytime SUHII difference between summer and winter (°C) and (B) average nighttime SUHII difference between summer and winter (°C) averaged over the period 2003–2008 across 419 global big cities. The two right plots beside (A) and (B) map are the latitudinal average of daytime and nighttime SUHII difference between summer and winter (°C), respectively. The black line indicates the average value, and the gray shaded areas are the uncertainty range indicated by mean \pm SD.

nighttime SUHII in the temperate regions over the Northern Hemisphere, and there are remarkable latitudinal variations in daytime SUHII (Figure 5). Mid-to-high latitude cities (e.g., Beijing, Vancouver) have larger seasonal amplitude of daytime SUHII than their low latitude sisters (Figure 5A). The evaporative cooling effects of the vegetation during the growing season may partly explain why the seasonal amplitude of heat islands differs between cities. For instance, the spatial distribution of the daytime SUHII seasonal amplitude is significantly correlated with the δ EVI seasonal amplitude (Figure 4; SI Figure S4); cities with a more seasonal greening contrast between urban area and suburban area also have a more seasonal urban heat island. As shown in SI Figure S6, tropical cities where vegetation is active all year round, show a flat seasonal profile of daytime SUHII throughout the year.

The nighttime SUHII exhibits a small summer to winter amplitude of less than 1 °C for more than 86% of the big cities (Figure 5B). The seasonal amplitude of nighttime SUHII is also more pronounced in cold regions (high latitudes) compared to warm regions (low latitudes). This variation is not explained by vegetation differences across cities ($R^2 = 0.02$ with δ VCF or $R^2 = 0.01$ with δ EVI; Figure 4B and Figure S5). However, the seasonal amplitude of nighttime SUHII negatively correlates with both the mean temperature for the months when air temperature exceeds 0 °C (MT0) and mean annual temperature ($R^2 = 0.26$, $P < 0.001$, and $R^2 = 0.15$, $P < 0.001$, respectively; Figure S5). This result is consistent with the larger solar radiation energy transformed into SUHII in summer over high latitude regions (Figure 4).³⁹

Although LST has different physical meanings from surface air temperature,⁴⁰ they have close and complex relation.

Generally under clear sky conditions, larger LST means larger sensible heat flux which could result in larger surface air temperature and higher urban boundary layer,^{13,14} while LST has larger diurnal amplitude than surface air temperature, and there is a time lag effect between them.⁴⁰ Likewise, surface urban heat island magnitude and diurnal amplitude is larger than that of air urban heat island.¹² In addition, it should be noted that although Wang et al. (2007)¹⁸ verified the accuracy of emissivities in MODIS LST products over Beijing city and Wan et al. (2008)¹⁶ tested MODIS LST products with ground LST measurement over lakes, grasslands, and agriculture fields, there is no comparison between direct ground urban LST measurements with MODIS LST products over urban regions yet. Future evaluation of MODIS LST products over urban regions is needed by urban heat island and other disciplinary studies.

Note that the 419 big cities with a population larger than 1 million¹⁹ include some large urban agglomerations (e.g., West Yorkshire) consisting of several smaller cities,²⁰ where the City Clustering Algorithm³⁰ defining urban area may have cause uncertainties of SUHII derived in this study. In addition, recent study has highlighted the importance of effects of climate conditions such as wind speed and cloud cover on the magnitude of the heat island effect at high spatiotemporal resolution.⁴¹ Such effects should be addressed in future studies when high spatiotemporal resolution data set on those climate variables become available.

In recent years, rapid global warming and extreme climate events have become one of the most urgent, yet complicated, issues facing both scientists and politicians. According to the recent report of IPCC,⁴² since the industrial revolution, global

land mean temperature increased by 0.84 ± 0.37 °C, and warm night frequency also increased. The large SUHII in summer not only undoubtedly increases the cooling power consumption in urban areas¹² but also could increase the risk of heatwave extreme events over urban areas, as urban areas are affected by both global and local climate forcing.⁴³ A big challenge presented to the scientists now is to separate the contribution of urbanization and global climate forcing (greenhouse gases increase, pollutants and aerosol concentration changes) to the urban temperature trends as well as urban extreme climate events and figure out how to adapt and mitigate serious heatwave events induced by climate change and urban heat island. At regional scale, fine-scale modeling studies^{44,45} will be necessary to understand the effects of urbanization on regional climate by accounting for urban-specific energy exchange properties, urban vegetation distribution, and ability to partition net radiation into latent or sensible heat.^{13,33,43} In addition, the magnitude of the daytime heat island seems to be significantly controlled by vegetation evaporative cooling. This adds another advantage to greener cities – better adaptation to climate change.

■ ASSOCIATED CONTENT

📄 Supporting Information

List of 419 big cities, detailed methods and figures for relationships between SUHII and explanation variables and spatial patterns of summer and winter SUHII. This material is available free of charge via the Internet at <http://pubs.acs.org>.

■ AUTHOR INFORMATION

Corresponding Author

*Phone: 86-10-6276-5578. Fax: 86-10-6275-6560. E-mail: slpiao@pku.edu.cn. Corresponding author address: Peking University, Beijing 100871, China.

■ ACKNOWLEDGMENTS

This study was supported by the National Natural Science Foundation of China (41125004 and 31021001).

■ ABBREVIATION LIST

BRDF, Bidirectional Reflectance Distribution Function
 BSA, black sky albedo
 CRU, Climate Research Unit
 EVI, Enhanced Vegetation Index
 IPCC, Intergovernmental Panel on Climate Change
 LST, land surface temperature
 MAP, mean annual precipitation
 MAT, mean annual temperature
 MODIS, MODerate-resolution Imaging Spectroradiometer
 MT0, mean air temperature for the months when air temperature exceeds 0 °C
 NDVI, Normalized Difference Vegetation Index
 NL, nighttime light
 NOAA, National Oceanic and Atmospheric Administration
 PD, population density
 VCF, vegetation cover fields
 WSA, white sky albedo

■ REFERENCES

(1) DeFries, R. Terrestrial Vegetation in the Coupled Human-Earth System: Contributions of Remote Sensing. *Annu. Rev. Environ. Resour.* **2008**, *33* (1), 369–390.

(2) Oke, T. R. The urban energy balance. *Prog. Phys. Geog.* **1988**, *12* (4), 471–508.

(3) Kalnay, E.; Cai, M. Impact of urbanization and land-use change on climate. *Nature* **2003**, *423* (6939), 528–531.

(4) Zhou, L. M.; Dickinson, R. E.; Tian, Y. H.; Fang, J. Y.; Li, Q. X.; Kaufmann, R. K.; Tucker, C. J.; Myneni, R. B. Evidence for a significant urbanization effect on climate in China. *Proc. Natl. Acad. Sci. U.S.A.* **2004**, *101* (26), 9540–9544.

(5) Jones, P. D.; Lister, D. H.; Li, Q. Urbanization effects in large-scale temperature records, with an emphasis on China. *J. Geophys. Res.* **2008**, *113*, D16122.

(6) Parker, D. E. Urban heat island effects on estimates of observed climate change. *Wiley Interdiscip. Rev.: Clim. Change* **2010**, *1* (1), 123–133.

(7) Fujibe, F. Detection of urban warming in recent temperature trends in Japan. *Int. J. Clim.* **2009**, *29* (12), 1811–1822.

(8) Stone, B. Urban and rural temperature trends in proximity to large US cities: 1951–2000. *Int. J. Clim.* **2007**, *27* (13), 1801–1807.

(9) Grimm, N. B.; Faeth, S. H.; Golubiewski, N. E.; Redman, C. L.; Wu, J.; Bai, X.; Briggs, J. M. Global Change and the Ecology of Cities. *Science* **2008**, *319* (5864), 756–760.

(10) National Bureau of Statistics. *China Statistical Yearbook*; China Statistics Press: Beijing, 2008.

(11) DeFries, R.; Pandey, D. Urbanization, the energy ladder and forest transitions in India's emerging economy. *Land Use Policy* **2010**, *27* (2), 130–138.

(12) Rizwan, A. M.; Dennis, L. Y. C.; Liu, C. A review on the generation, determination and mitigation of Urban Heat Island. *J. Environ. Sci.* **2008**, *20* (1), 120–128.

(13) Arnfield, A. J. Two decades of urban climate research: A review of turbulence, exchanges of energy and water, and the urban heat island. *Int. J. Climatol.* **2003**, *23* (1), 1–26.

(14) Voogt, J. A.; Oke, T. R. Thermal remote sensing of urban climates. *Remote Sens. Environ.* **2003**, *86* (3), 370–384.

(15) Imhoff, M. L.; Zhang, P.; Wolfe, R. E.; Bounoua, L. Remote sensing of the urban heat island effect across biomes in the continental USA. *Remote Sens. Environ.* **2010**, *114* (3), 504–513.

(16) Wan, Z. New refinements and validation of the MODIS Land-Surface Temperature/Emissivity products. *Remote Sens. Environ.* **2008**, *112* (1), 59–74.

(17) Hung, T.; Uchihama, D.; Ochi, S.; Yasuoka, Y. Assessment with satellite data of the urban heat island effects in Asian mega cities. *Int. J. Appl. Earth Obs. Geoinf.* **2006**, *8*, 34–48.

(18) Wang, K.; Wang, J.; Wang, P.; Sparrow, M.; Yang, J.; Chen, H., Influences of urbanization on surface characteristics as derived from the Moderate-Resolution Imaging Spectroradiometer: A case study for the Beijing metropolitan area. *J. Geophys. Res.* **2007**, *112* (D22), doi: 10.1029/2006jd007997.

(19) United Nations, *World Urbanization Prospects: The 2007 Revision*, 2008.

(20) Available at: <http://www.geonames.org> (accessed August 10, 2009).

(21) Friedl, M. A.; McIver, D. K.; Hodges, J. C. F.; Zhang, X. Y.; Muchoney, D.; Strahler, A. H.; Woodcock, C. E.; Gopal, S.; Schneider, A.; Cooper, A.; Baccini, A.; Gao, F.; Schaaf, C. Global land cover mapping from MODIS: algorithms and early results. *Remote Sens. Environ.* **2002**, *83* (1–2), 287–302.

(22) Hansen, M. C.; Defries, R. S.; Townshend, J. R. G.; Carroll, M.; Dimiceli, C.; Sohlberg, R. A. Global percent tree cover at a spatial resolution of 500 meters: First results of the MODIS vegetation continuous fields algorithm. *Earth Interact.* **2003**, *7*, 1–15.

(23) Huete, A.; Didan, K.; Miura, T.; Rodriguez, E. P.; Gao, X.; Ferreira, L. G. Overview of the radiometric and biophysical performance of the MODIS vegetation indices. *Remote Sens. Environ.* **2002**, *83*, 195–213.

(24) Schaaf, C. B.; Gao, F.; Strahler, A. H.; Lucht, W.; Li, X. W.; Tsang, T.; Strugnell, N. C.; Zhang, X. Y.; Jin, Y. F.; Muller, J. P.; Lewis, P.; Barnsley, M.; Hobson, P.; Disney, M.; Roberts, G.; Dunderdle, M.; Doll, C.; d'Entremont, R. P.; Hu, B. X.; Liang, S. L.; Privette, J. L.; Roy,

D. First operational BRDF, albedo nadir reflectance products from MODIS. *Remote Sens. Environ.* **2002**, *83*, 135–148.

(25) Mitchell, T. D.; Jones, P. D., An improved method of constructing a database of monthly climate observations and associated high-resolution grids. *Int. J. Climatol.* **2005**, *25*, 693–712. Available at: <http://badc.nerc.ac.uk/data/cru/> (accessed November 8, 2007).

(26) Center for International Earth Science Information Network (CIESIN). *Gridded Population of the World, version 3 (GPWv3)*; 2010. Available at: <http://sedac.ciesin.columbia.edu/gpw/> (accessed August 10, 2009).

(27) Doll, C. H.; Muller, J.-P.; Elvidge, C. D. Night-time Imagery as a Tool for Global Mapping of Socioeconomic Parameters and Greenhouse Gas Emissions. *AMBIO* **2000**, *29* (3), 157–162.

(28) Elvidge, C. D.; Baugh, K. E.; Kihn, E. A.; Kroehl, H. W.; Davis, E. R.; Davis, C. W. Relation between satellite observed visible-near infrared emissions, population, economic activity and electric power consumption. *Int. J. Remote Sens.* **1997**, *18* (6), 1373–1379.

(29) Elvidge, C. D.; Erwin, E. H.; Baugh, K. E.; Ziskin, D.; Tuttle, B. T.; Ghosh, T.; Sutton, P. C. In *Overview of DMSP nighttime lights and future possibilities*, Urban Remote Sensing Event, 2009 Joint, 20–22 May 2009; pp 1–5.

(30) Rozenfeld, H. D.; Rybski, D.; Andrade, J. S.; Batty, M.; Stanley, H. E.; Makse, H. A. Laws of population growth. *Proc. Natl. Acad. Sci.* **2008**, *105* (48), 18702–18707.

(31) Ricker, W. E. Linear regressions in fisheries research. *J. Fish. Res. Board Can.* **1973**, *30*, 409–434.

(32) Stabler, L. B.; Martin, C. A.; Brazel, A. J. Microclimates in a desert city were related to land use and vegetation index. *Urban Forestry Urban Greening* **2005**, *3* (3–4), 137–147.

(33) Grimmond, C. S. B. The suburban energy balance: methodological considerations and results for a mid-latitude west coast city under winter and spring conditions. *Int. J. Clim.* **1992**, *12* (5), 481–497.

(34) Weng, Q. H.; Lu, D. S.; Schubring, J. Estimation of land surface temperature-vegetation abundance relationship for urban heat island studies. *Remote Sens. Environ.* **2004**, *89* (4), 467–483.

(35) Hu, Y.; Jia, G. Influence of land use change on urban heat island derived from multi-sensor data. *Int. J. Climatol.* **2010**, *30* (9), 1382–1395.

(36) Taha, H. Urban climates and heat islands: Albedo, evapotranspiration, and anthropogenic heat. *Energy Build.* **1997**, *25* (2), 99–103.

(37) Sailor, D. J. A review of methods for estimating anthropogenic heat and moisture emissions in the urban environment. *Int. J. Climatol.* **2011**, *31* (2), 189–199.

(38) Rizwan, A. M.; Dennis, L. Y. C.; Liu, C. An investigation of urban heat island intensity (UHII) as an indicator of urban heating. *Atmos. Res.* **2009**, *94* (3), 491–500.

(39) Wilby, R. L. Past and projected trends in London's urban heat island. *Weather* **2003**, *58*, 251–260.

(40) Jin, M.; Dickinson, R. E. Land surface skin temperature climatology: benefitting from the strengths of satellite observations. *Environ. Res. Lett.* **2010**, *5* (4), 044004.

(41) Tomlinson, C. J.; Chapman, L.; Thornes, J. E.; Baker, C. J. Derivation of Birmingham's summer surface urban heat island from MODIS satellite images. *Int. J. Climatol.* **2010**, DOI: 10.1002/joc.2261.

(42) IPCC. *Climate Change 2007: The Physical Science Basis*; Cambridge Univ. Press: Cambridge, U.K., 2007.

(43) McCarthy, M. P.; Best, M. J.; Betts, R. A. Climate change in cities due to global warming and urban effects. *Geophys. Res. Lett.* **2010**, *37* (9), L09705.

(44) Oleson, K. W.; Bonan, G. B.; Feddema, J.; Vertenstein, M. An urban parameterization for a global climate model. Part II: Sensitivity to input parameters and the simulated urban heat island in offline Simulations. *J. Appl. Meteorol. Climatol.* **2008**, *47*, 1061–1076.

(45) Oleson, K. W.; Bonan, G. B.; Feddema, J. Effects of white roofs on urban temperature in a global climate model. *Geophys. Res. Lett.* **2010**, *37*, L03701.